European Multidisciplinary Journal of Modern Science

Vol. 26 **Issue** 3 | **pp.** 22-21 | **ISSN:** 2750-6274
Available online @ https://emjms.academicjournal.io

ACADEMIC JOURNAL

Preparation and Study of Structural and Optical Properties of PbS:Cu Nanostructured Thin Films

Hiba Jumaa Jaafer[1*]

[1] Department of Science, College of Basic Education, University of Diyala, Baquba, Iraq
* Correspondence: jafeer.hiba@gmail.iq

Abstract:
Thin films of lead sulfide (PbS) and various Cu mixing ratios (30%, 50%, and 70%) are used in this work. were made using the (PLD) method on glass substrates at a wavelength of 1064 nm and 600 mj of laser energy. X-ray diffraction experiments were used to determine the structural measurements for pure PbS, and other mixes present thin films demonstrated a face-centered-cubic structure. and discovered that the average grain size was 17.74 nm; this grew to 20.54 nm after combining with 30% Cd, 20.54 nm after mixing with 50% Cd, and 23.15 nm after mixing with 70% Cd. The optical characteristics of PbS thin films measured between 300 and 1100 nm in wavelength. For PbS thin films, the optical transmittance and transparency decrease as the o mixing ratio increases.The absorption coefficient rises as the mixing ratio does. When the mixing ratio is increased, the band gap for pure PbS thin film is 2.43, rises to 3.03, and thereafter falls to 2.01 and 1.5.

Keywords: lead sulphide, pulsed laser deposited, xrd diffraction, optical properties, electrical properties

Citation: Jaafer, H.J. Preparation and Study of Structural and Optical Properties of PbS:Cu Nanostructured Thin Films. *European Multidisciplinary Journal of Modern Science*. **2024**, 26(3), 22-21.

Received: 21 February 2024
Revised: 28 February 2024
Accepted: 7 March 2024
Published: 14 March 2024

1. Introduction

At ambient temperature, the narrow band gap of lead sulfide (PbS), a direct band gap semiconductor, is 0.4 eV [1]. Semiconductor materials, which are IV-VI compound semiconductors, are currently well positioned in solid state technology and research [2]. It has been observed that reducing the grain size to the Nano regime can extend the band gap to as high as 2.5 eV from its bulk value. Modifying the grain size of PbS can significantly alter the band gap [3]. By adjusting different preparation conditions, PbS thin film optical band gap may be set to 1.5 eV and electrical resistivity can be reduced [4,5]. These traits have been connected to substrate types and growth conditions. Due to these factors, a number of research teams are interested in creating and examining this material using a variety of deposition techniques, including chemical bath deposition (CBD), spray pyrolysis, photo-accelerated chemical deposition, and microwave heating. [6]. One of the newest and most advanced methods for thin film deposition is pulsed laser deposition (PLD).

Cu is a reddish-brown, ductile, malleable, highly conductive metal that resists corrosion. It is typically found in metal ores that also contain carbonates, sulphides, arsenides, and chlorides.Cu is mostly utilized in electrical and plumbing conductors. Cu oxidizes slowly in air, and a coating of Cu2 (OH)2CO3 causes Cu to become green on its surface when CO2 is present. It often appears in the form of +2 oxidation. CuO is the black form of copper (II) oxide, which can also exist in the +1 state. Cu2O stands for red copper (I) oxide. Although excessive levels of copper are hazardous, trace amounts are necessary for life because they play a significant part in the operation of enzymes as co-

enzymes [7].

2. Method

2.1. Experimental procedure

Pbs thin films are made by the PLD technique. The experiment was carried out at a pressure of 10-3 Torr in a vacuum chamber. Using PbS from Fluka Chemical (Germany), the target was produced into a disk with a diameter of 1 cm and a thickness of 0.3 cm using a hydraulic piston type (SPECAC) and 6 tons of pressure for 10 minutes. Cu element was combined with these components at a purity of 98% in various present-day situations. It must be as uniform and dense as possible to guarantee a high-quality deposit. Because it greatly affects the characteristics of the films deposited on it, the substrate's nature is crucial. The quality of adherence of deposited films is highly dependent on the effectiveness of substrate cleaning. In this work, the structural and optical properties of PbS layers were investigated using glass slides. the laser configuration, which displays the target and substrate positions inside the chamber with respect to the laser beam. One kind of laser that uses Nd: Y is the Nd: YAG laser (Huafei Tongda Technology- DIAMOND-288 pattern EPLS) 600 m J of power, 6 Hz of frequency, and 1064 nm of wavelength 100 pulses equals one shot. A focused Nd: YAG SHG Q-switching laser's incident beam angles itself at 45° with the target surface as it enters via a window.

3. Results and Discussion

The cubic crystal system of pure PbS thin films, which were produced on a glass substrate using a Cu – 0.15406 nm laser source, was revealed by the XRD diffraction diagnostic data. The X-ray diffraction pattern (XRD) of pure lead(II) sulfide before and after mixing with (0.3,0.5,0.7) Cd is shown in Figure (1). X-rays having diffraction peaks of the International Center for Diffraction Data (ICDD) number (01 - 078 - 1055) were present. The great purity and evident crystallization of the PbS film in pure PbS are in line with the findings of M. Cheraghizade and colleagues' research [15]. The diffraction pattern also revealed that the primary growth trends are (2 2 2) and (1 3 3), respectively, and that the peak intensity appeared at ($2m$ = 53.6163 and 69.077). Using the Debye-Scherer equation, the crystal size (D) of the X-ray diffraction pattern for each sample was determined. The Pure PbS sample's crystal size was determined to be 17.74 nm. Thin films of PbS combined with 0.3Cu revealed a cubic crystal structure through XRD analysis. X-rays bearing the International Center for Diffraction Data (ICDD) number (01 - 078 - 1898) diffraction peaks.

The X-ray diffraction pattern (XRD) of PbS combined with 0.3Cu is displayed in Figure (1). The film's exceptional clarity and crystallization are evident. Additionally, the diffraction pattern revealed that the primary growth trend is (2 2 2) and that the high intensity arrived at (2⌾= 53.5115). In addition, one peak of Cu was seen in the diffraction pattern at (2⌾ = 74.1031), in accordance with the international standard card number (96 - 901 - 3015). The PbS combined with 0.3Cu sample has a crystal size of 20.54 nm. However, regarding (XRD) of PbS combined with 0.5Cu concentration. The film's exceptional clarity and crystallization are evident. Additionally, the diffraction pattern revealed that the primary growth trend is (2 2 2) and that the high intensity arrived at (2⌾= 53.5115). One peak of Cu was also visible in the diffraction pattern at (2⌾ = 74.1031),. The international standard card number (96 - 901 - 3015) indicates that the intensity is higher than that of Cu peaks at a concentration of 0.3. The PbS sample doped with 0.5Cu has a crystal size of 20.54 nm.

Regarding PbS (XRD) with a 0.7Cu mixing concentration, the film's exceptional clarity and crystallization are evident. Additionally, the diffraction pattern revealed that the primary growth trend is (2 2 2) and that the high intensity arrived at (2⌾= 53.5115). In

addition, one peak of Cu was seen in the diffraction pattern at (2⊚ = 74.1031), in accordance with the international standard card number (96 - 901 - 3015). The PbS combined with 0.7Cu sample has a crystal size of (23.15nm).

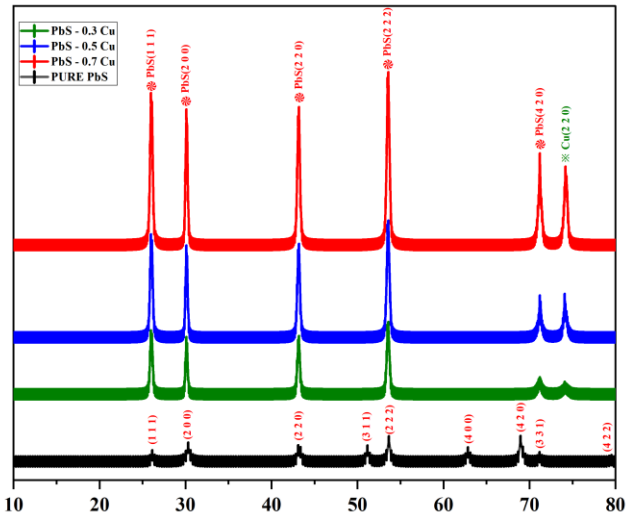

Figure 1. X-ray diffraction pattern of pure PbS and mixed with (0.3,0.5,0.7)Cu thin film prepared on a glass substrate

Figure 2A-2D shows FESEM micrographs of pure and mixed films. They display FESEM micrographs of nanocrystalline pure and mixed (PbS: Cu) thin films at 10 kx and 20 kx magnifications. The compact, polycrystalline, cauliflower-like nano crystallite particles were seen in an uneven distribution over the scanned area, as shown in Figure 2A.

The FESEM pictures in Figure 2B demonstrate that as the Cu ratio increases, the particle grain size decreases. Furthermore, the pure PbS film's surface was uniform and covered in a dense layer of nanocrystallites that resembled cauliflowers. These crystals seem to be randomly orientated, exhibit unusual forms, and have a varied size distribution. Nucleation and coalescence were suggested as the causes of the change in particle size and form.Grain growth is generally changed by nucleation and coalescence, which shift grain boundaries. The primary variables that affect this process are the kind of solvent, the concentration of the solution, the feed rate of the solution, the deposition temperature, and the composition of the precursor materials.

The thin film's surface, depicted in Figure 2C, has a morphology made up of tightly packed particles without any visible pinholes or fractures. It is possible to trace the coalescence to the incorporation of Cu+ ions during growth. Therefore, it can be hypothesized that Cu in the sample improved surface diffusion in relation to the precursor's incoming flux. Furthermore, the morphology showed spherical or cauliflower-like forms.

Figure 2D demonstrates how the surface shape and density of the produced film with 70% Cu mixture caused discernible alterations. Furthermore, the pictures showed agglomerations of nanoparticles in a variety of sizes and shapes, including spherical and cauliflower.

All thin films, pure and mixed, have their crystallite sizes entered into Table 1.

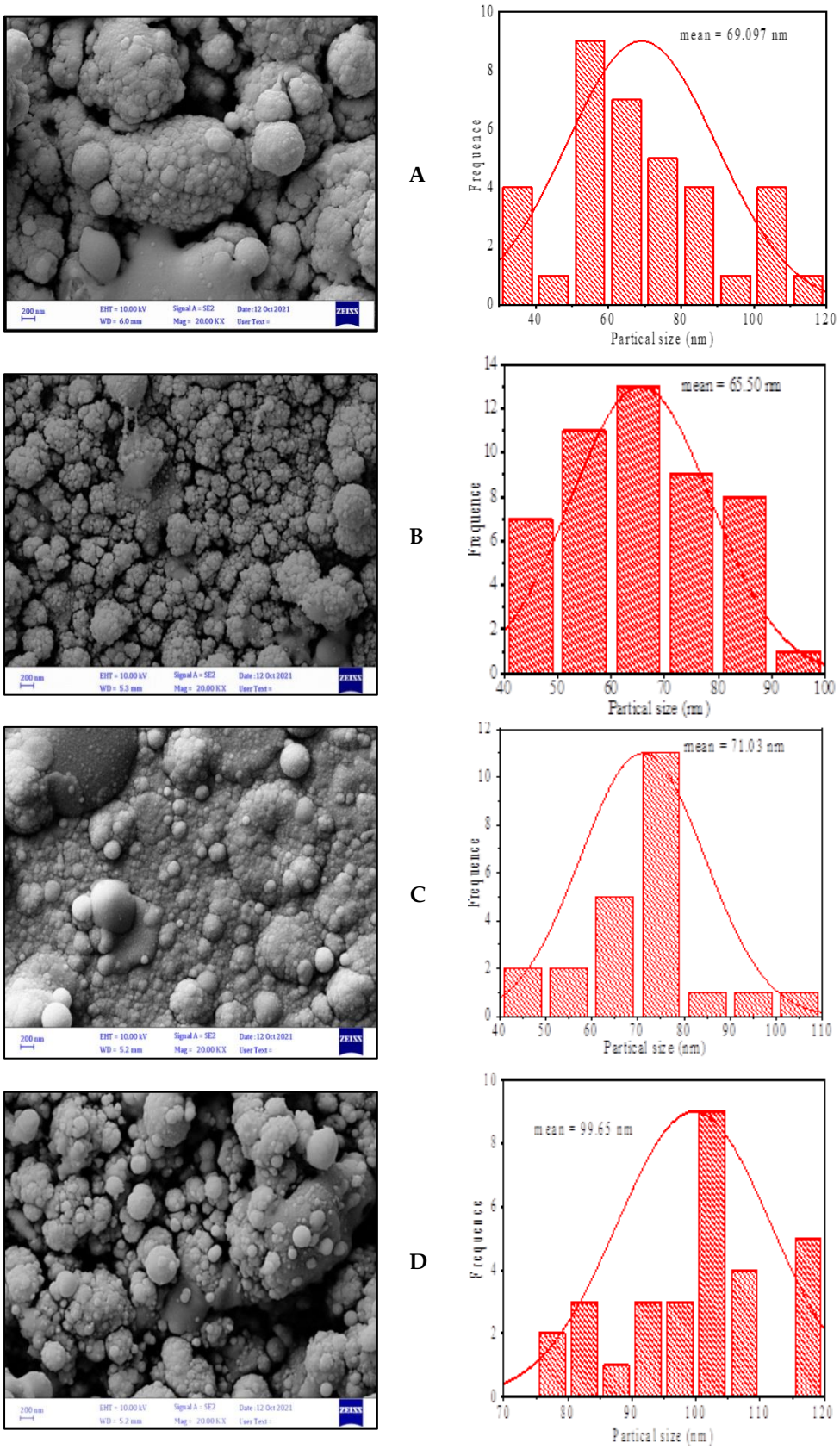

Figure 2. FESEM images and Histogram of (A) pure PbS and mixed with (B) 30% Cu thin films (C) 50% Cu thin films (D) 70% Cu thin films

Table 1. Crystallites size of prepared samples.

Samples	Crystallite Size (nm)
PbS	71.2
PbS: 30% Cu	69
PbS: 50% Cu	70
PbS: 70% Cu	98.2

Figure 3 (a-d) displays the EDX spectra of pure (PbS) and Cu-mixed PbS thin films at different ratios. Table displays the quantitative studies of the synthetic films' chemical composition (2). Pb, S, and Cu elements are unmistakably present in the pure and mixed samples, according to the EDS spectra. The high level of purity of each prepared sample is shown in the figure and table. Additionally, it was observed that when the mixing ratio dropped, the amounts of Pb and S grew and the amounts of Cu decreased.

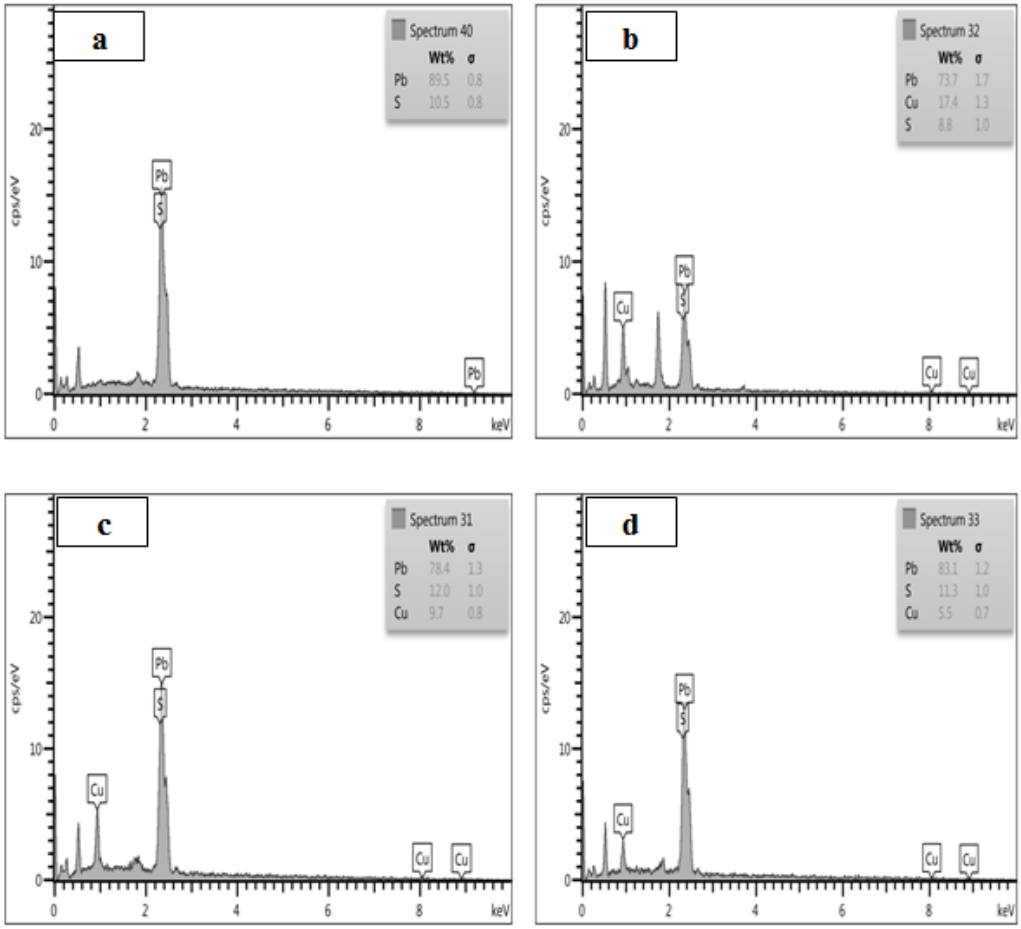

Figure 3. EDS of the pure and PbS mixed Cu thin films at (a) pure, (b) 30%, (c) 50% and (d) 70%.

Table 2. Pb, S and Cu concentration in PbS, and PbS: Cu samples with various mix ratios

Samples	Atomic concentration (%)		
	Pb	S	Cu
PbS	89.5	10.5	0
PbS: 30% Cu	73.7	8.8	17.4
PbS: 50% Cu	78.4	12	9.7
PbS: 70% Cu	83.1	11.3	5.5

The created pure and mixed thin film morphologies on glass substrates have changed, according to an AFM investigation. Figure 4 (a-d) displays the histogram diagram and 3D AFM pictures of the surface morphology taken on samples of the deposited PbS and PbS mixed Cu thin films. The average grain size, roughness, and RMS roughness are the three AFM metrics. Table 3 shows the data of the observed results for synthesized samples. In every instance, a thick surface of the thin films was achieved. The grains in the thin sheets were stacked. The average values of grain size appeared to fall from (36.74-35.8) nm with increasing Cu ratio from (0 to 30%) and subsequently increase from (56.23-368.4) nm with increasing Cu ratio from (50 to 70%) according to AFM pictures that displayed the PbS grain size as a function of varied mixing ratios. Additionally, it has been noted that there is a similar relationship between the mixing ratio, RMS, and average roughness.

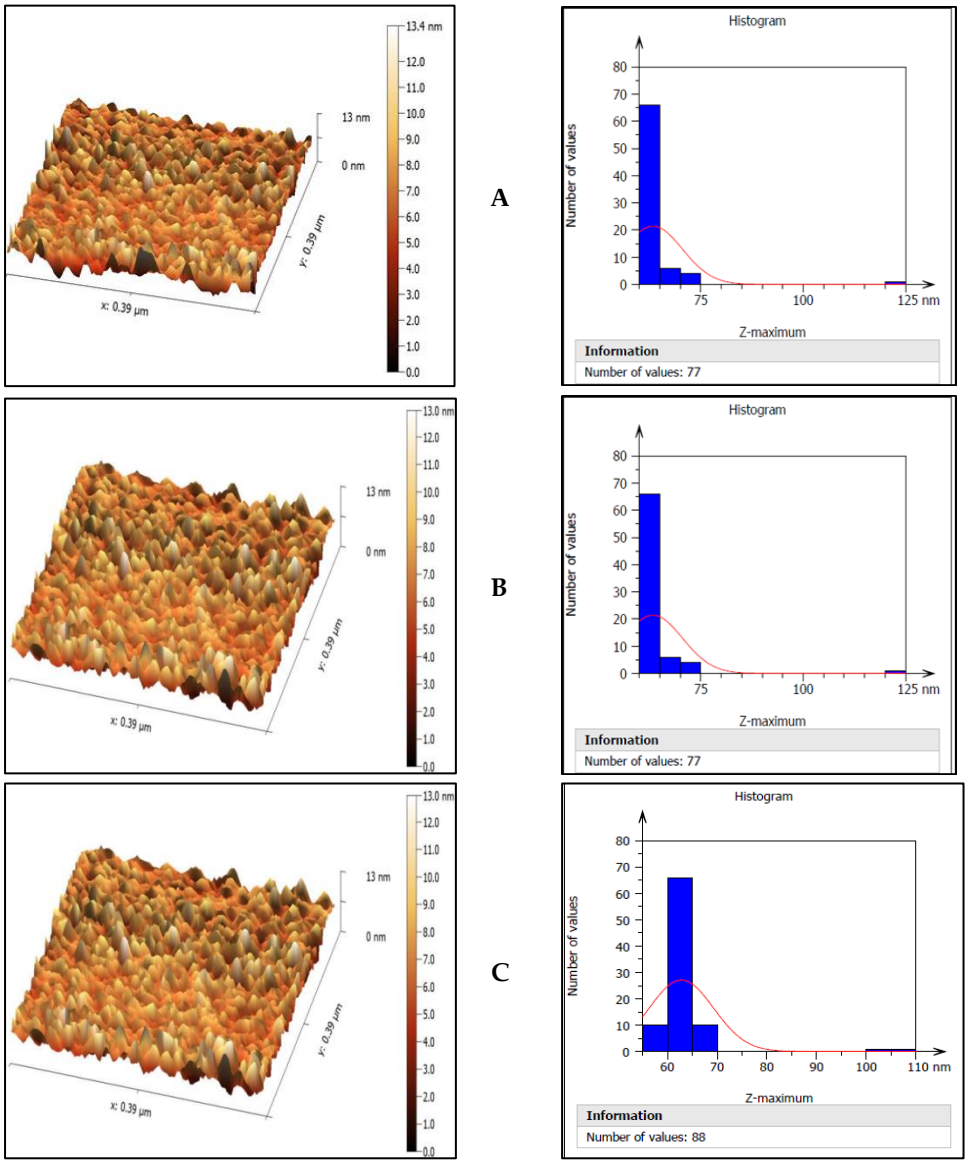

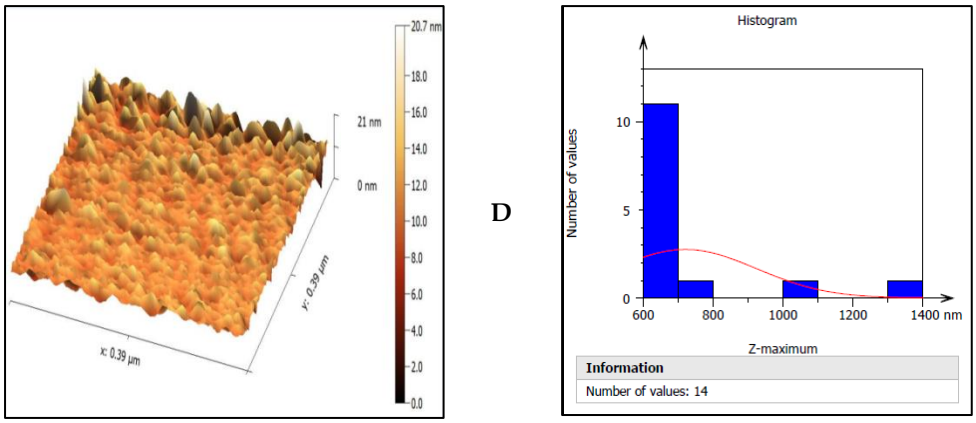

Figure 4. 3D AFM images and histogram for PbS and mixed thin films of different ratios of Cu (A) pure, (B) 30%, (C) 50% and (D) 70%.

Table 3. Pb, S and Cu concentration in PbS, and PbS: Cu samples with various mix ratios

Samples	Surface Roughness (nm)	RMS (nm)	Grain Size (nm)
PbS	15.32	18.03	36.74
PbS: 30% Cu	10.36	12.72	35.80
PbS: 50% Cu	13.14	18.11	56.23
PbS: 70% Cu	124.2	157.2	368.4

The transmittance spectra of the pure PbS film and the cooper-mixed films at 30%, 50%, and 70% ratios are displayed in Figure (5). At lower wavelengths, the transmittance of all thin films increases with wavelength, whereas at higher wavelengths, it increases slowly. The visible and infrared portions of the spectrum have high transmittance, while the ultraviolet area exhibits poor transmittance. The majority of the samples exhibit a visible region window, which is advantageous for solar cell applications. At 900 nm wavelength, the transmittance of the materials under study increases from 25% to 70%. Additionally, it was discovered that when the mixing ratio increased, the transmittance % decreased. Furthermore, a maximum transmittance of almost 68% was noted for mixed thin films with a 30% ratio.

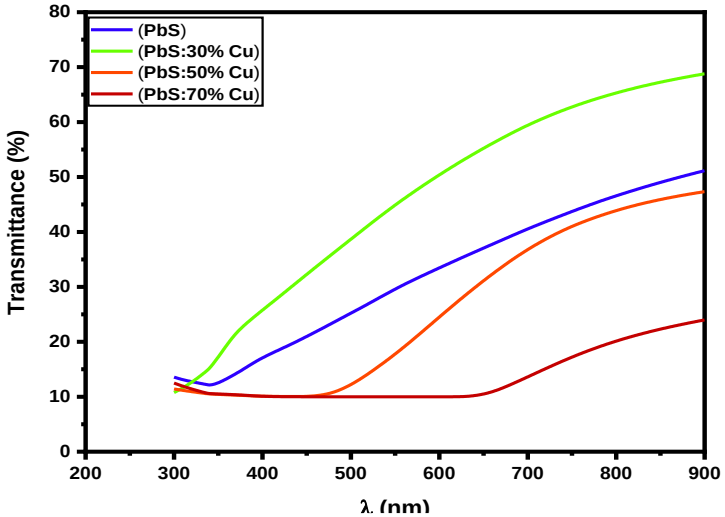

Figure 5. Transmittance versus wavelength of pure and mixed thin films at different ratios of Cu.

The absorbance spectra of the pure PbS film and the cooper-mixed films with the ratios of 30%, 50%, and 70% is displayed as a function of wavelengths (300-900 nm) in Figure 6. It was observed that the absorbance responds in the opposite way to the transmittance, peaking at 300 nm and subsequently falling down as the wavelength increases until stabilizing around 900 nm, as the image illustrates. It was seen from the spectrum that the absorbance rises as the mixing ratio rises. When the incident photon's energy is equal to or less than the energy gap value, the absorbance drops at long wavelengths (low energies) that correspond to the film's energy gap. Because the incident photon's value is bigger than the semiconductor's energy gap, this indicates that the photon was physically significant in causing the electron to become irritated and move from the valence band to the conduction band.

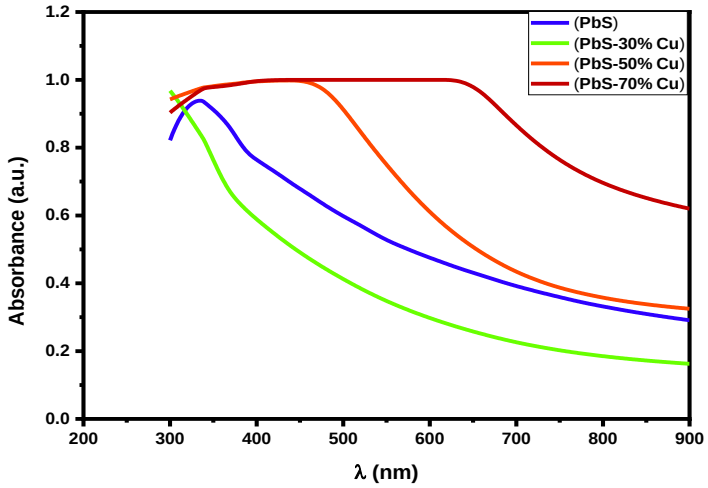

Figure 6. Absorbance versus wavelength of pure and mixed thin films at different ratios of Cu

The absorption coefficient value in Figure (7) illustrates the variation in the absorption coefficient (α) with respect to photon energy (hv) for three different ratios of PbS:Cu and pure lead sulfide films (30%, 50%, and 70%), which were created using the laser ablation method. It is evident from the figure that the absorption edge is not crisp, which could be because to the polycrystalline films' structure. It was observed in the same figure that as the mixing ratio increased, the absorption coefficient's value generally increased at the energy of the gap, indicating a decrease in the energy gap. The figure also showed that, at low energies, there is little change in the absorption coefficient values with photon energy. However, at energies between 1.5 and 4.2 eV, there is a significant change, and this rapid increase in absorption coefficient values ($\alpha > 104$ cm-1) aids in the prediction of direct electronic transmissions.

Table 4. Energy gap for pure film and mixed films by different ratios of Cu

Sample	PbS (pure)	(PbS:30% Cu)	(PbS:50% Cu)	(PbS:70% Cu)
E_g	2.43	3.03	2.01	1.5

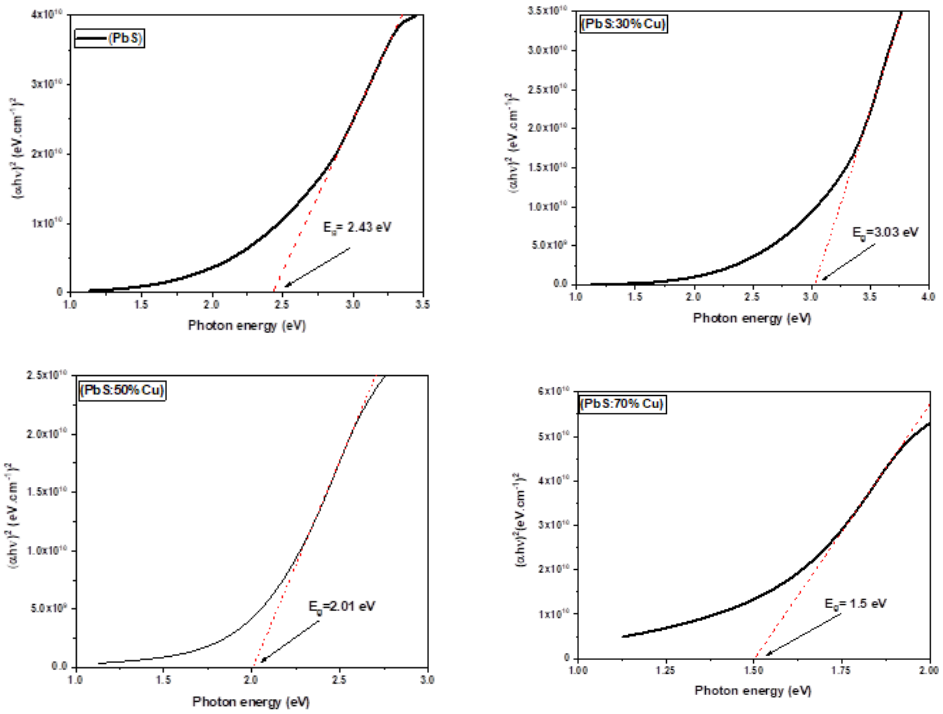

Figure 8. The relation between (αhυ)2 and (hυ) of pure and mixed thin films at different ratios of Cu

Hall effect measurement is utilized to calculate the majority of electrical carriers' type, carrier concentration (nH), and hall mobility (μH) for pure PbS thin films and its combination with Cu at varied ratios that were formed at room temperature using laser induce method on glass substrates. The hall mobility (μH), carrier concentration (nH), and hall coefficient values. Table (5) displays the variations in the carrier's concentration (nH) and hall mobility (μH) of PbS pure and mixed films with (Cu). According to the Hall effect data, every movie is (p-type). The Table made it evident that when PbS:Cu was mixed, there was a drop in carrier concentration and an increase in carrier mobility (μH). This is because the disordered state of the crystal lattice is reducing, leading to a reduction in phonon and ionized impurity scattering as well as a drop in mobility.

Table 5. Hall parameters of (PbS) Pure and mixed films with different ratios of Cd, Cu and Co

Samples	RH × 103 (cm3/C)	nH ×1015 (cm)-3	μH × 103 (cm2/V.sec)	Type
PbS	1.45	4.29	2.68	P
PbS:Cd	4.25	1.47	14.6	P
PbS:Cu	0.863	4.24	2.79	P
PbS:Co	7.38	8.46	46.4	P

4. Conclusion

In conclusion, this study has successfully demonstrated the preparation and characterization of PbS:Cu nanostructured thin films. Through various techniques such as chemical bath deposition and structural analysis using X-ray diffraction, the films' structural properties were thoroughly examined, revealing their crystalline nature and preferred orientation. Additionally, optical properties were investigated through UV-Vis spectroscopy, elucidating the films' absorption behavior and bandgap energy. The incorporation of copper (Cu) dopant was found to influence the films' structural and optical properties, offering insights into potential applications in optoelectronic devices. Overall, this research contributes to the understanding of nanostructured thin films and

their potential for use in various technological applications, paving the way for further exploration and development in this field.

References

[1] D. A. Jameel, "Thin Film Deposition Processes," *Int. J. Mod. Phys. Appl.*, vol. 1, no. 4, pp. 193–199, 2015.

[2] F. Göde, E. Güneri, F. M. Emen, V. Emir Kafadar, and S. Ünlü, "Synthesis, structural, optical, electrical and thermoluminescence properties of chemically deposited PbS thin films," *J. Lumin.*, vol. 147, pp. 41–48, Mar. 2014, doi: 10.1016/j.jlumin.2013.10.050.

[3] P. Patnaik, *Handbook of inorganic chemicals*, vol. 529. McGraw-Hill New York, 2003.

[4] Y. Wang, A. Suna, W. Mahler, and R. Kasowski, "PbS in polymers. From molecules to bulk solids," *J. Chem. Phys.*, vol. 87, no. 12, pp. 7315–7322, Dec. 1987, doi: 10.1063/1.453325.

[5] R. Bai, D. Kumar, S. Chaudhary, and D. K. Pandya, "Highly crystalline p-PbS thin films with tunable optical and hole transport parameters by chemical bath deposition," *Acta Mater.*, vol. 131, pp. 11–21, 2017, doi: https://doi.org/10.1016/j.actamat.2017.03.062.

[6] B. Touati, A. Gassoumi, I. Dobryden, M. M. Natile, A. Vomiero, and N. K. Turki, "Superlattices," *Microstruct*, vol. 97, pp. 519–528, 2016.

[7] K. Al Akeel, "Empirical Investigation of Water Pollution Control through Use of Phragmites australis," Brunel University, 2013.